

# Metabolite profiling of red and blue potatoes revealed cultivar and tissue specific patterns for anthocyanins and other polyphenols

Anne Oertel<sup>1,2</sup> · Andrea Matros<sup>2</sup> · Anja Hartmann<sup>2</sup> · Panagiotis Arapitsas<sup>4</sup> · Klaus J. Dehmer<sup>3</sup> · Stefan Martens<sup>1,4</sup> · Hans-Peter Mock<sup>2</sup>

Received: 2 January 2017 / Accepted: 26 May 2017 / Published online: 29 June 2017  
© Springer-Verlag GmbH Germany 2017

## Abstract

**Main conclusion** Metabolite profiling of tuber flesh and peel for selected colored potato varieties revealed cultivar and tissue specific profiles of anthocyanins and other polyphenols with variations in composition and concentration.

Starchy tubers of *Solanum tuberosum* are a staple crop and food in many countries. Among cultivated potato varieties a huge biodiversity exists, including an increasing number of red and purple colored cultivars. This coloration relates to the accumulation of anthocyanins and is supposed to offer nutritional benefits possibly associated with the antioxidative capacity of anthocyanins. However, the anthocyanin composition and its relation to the overall polyphenol constitution in colored potato tubers have not been investigated closely. This study focuses on the

phytochemical characterization of the phenolic composition of a variety of colored potato tubers, both for peel and flesh tissues. First, liquid chromatography (LC) separation coupled to UV and mass spectrometry (MS) detection of polyphenolic compounds of potato tubers from 57 cultivars was used to assign groups of potato cultivars differing in their anthocyanin and polyphenol profiles. Tissues from 19 selected cultivars were then analyzed by LC separation coupled to multiple reaction monitoring (MRM) to detect quantitative differences in anthocyanin and polyphenol composition. The measured intensities of 21 anthocyanins present in the analyzed potato cultivars and tissues could be correlated with the specific tuber coloration. Besides secondary metabolites well-known for potato tubers, the metabolic profiling led to the detection of two anthocyanins not described for potato tuber previously, which we tentatively annotated as pelargonidin feruloyl-xylosyl-glucosyl-galactoside and cyanidin 3-*p*-coumaroylrutinoside-5-glucoside. We detected significant correlations between some of the measured metabolites, as for example the negative correlation between the main anthocyanins of red and blue potato cultivars. Mainly hydroxylation and methylation patterns of the B-ring of dihydroflavonols, leading to the formation of specific anthocyanidin backbones, can be assigned to a distinct coloring of the potato cultivars and tuber tissues. However, basically the same glycosylation and acylation reactions occur regardless of the main anthocyanidin precursor present in the respective red and blue/purple tissue. Thus, the different anthocyanin profiles in red and blue potato cultivars likely relate to superior regulation of the expression and activities of hydroxylases and methyltransferases rather than to differences for downstream glycosyl- and acyltransferases. In this regard, the characterized potato cultivars represent a valuable resource for the molecular analysis of the genetic

**Electronic supplementary material** The online version of this article (doi:10.1007/s00425-017-2718-4) contains supplementary material, which is available to authorized users.

✉ Hans-Peter Mock  
mock@ipk-gatersleben.de

- <sup>1</sup> TRANSMIT GmbH, Project Division: PlantMetaChem (PMC), Kerkrader Straße 3, 35394 Giessen, Germany
- <sup>2</sup> Department of Physiology and Cell Biology, Leibniz Institute of Plant Genetics and Crop Plant Research (IPK-Gatersleben), Corrensstraße 3, 06466 Stadt Seeland OT Gatersleben, Germany
- <sup>3</sup> Leibniz Institute of Plant Genetics and Crop Plant Research (IPK), Genebank Department/GLKS, Parkweg 3a, 18190 Gross Luesewitz, Germany
- <sup>4</sup> Department of Food Quality and Nutrition, Edmund Mach Foundation, Research and Innovation Centre, Via E. Mach 1, 38010 San Michele all'Adige (TN), Italy

background and the regulation of anthocyanin side chain modification.

**Keywords** Colored potatoes · Flavonoids · LC–MS/MS · Metabolomics · *Solanum tuberosum* L

### Abbreviations

ESI	Electrospray ionization
MRM	Multiple reaction monitoring
PCA	Principal component analysis
PDA	Photodiode array
TQMS	Triple quadrupole mass spectrometry
UHR-TOF-MS	Ultra-high resolution time-of-flight mass spectrometry
UPLC	Ultra-performance liquid chromatography

### Introduction

Anthocyanins are glycosidic water soluble pigments, belonging to the group of flavonoids, which give many fruits and flowers a red to purple or blue coloration. Their water solubility is due to a glycosidic bound sugar residue, whereas the color is attributed to the aglycone (anthocyanidin) (Castaneda-Ovando et al. 2009). Six major anthocyanidins are naturally occurring, which are petunidin, pelargonidin, cyanidin, peonidin, malvidin and delphinidin. Currently, a range of 700 anthocyanins have been identified, differing in their overall hydroxylation pattern, in methylation, glycosylation and acylation, and consequently in their coloration (He and Giusti 2010). The color variation is due not only to the global pigment concentration but also to the proportion of different types of pigments and their secondary modifications, which can affect the stability and reactivity of anthocyanins and the chromatic properties of the pigments (Fournier-Level et al. 2011).

There is an increasing interest in anthocyanins (Bridle and Timberlake 1997) since these pigments fulfill several protective functions in plants. They protect plant DNA and proteins against UV-induced damages (Steyn et al. 2002), which are involved in defense against diverse biotic and abiotic stresses (Chalker-Scott 1999; Wegener and Jansen 2007), show antioxidant capacity and help to attract potential pollinators (Xie et al. 2015). Furthermore, anthocyanins are potentially beneficial for human health (He and Giusti 2010; Lila 2004). For a number of anthocyanins antioxidant, anti-carcinogenic (Bagchi et al. 2004; Butelli et al. 2008) and anti-inflammatory (Ohgami et al. 2005) activities have been shown, as well as a possible support of diabetes prevention and treatment (Tsuda 2016) and heart health (Mazza 2007).

Potato, belonging to the genus *Solanum*, is among the most important staple foods worldwide. Thus, pigmented varieties may provide a major quantitative source of anthocyanins with aforementioned nutritional health benefits (Prior 2003). Increasing interest in anthocyanin-rich colored potatoes as ‘functional food’ from the food industry, nutritional science and consumers gained the attention of potato breeders. Providing new information about phytochemical characteristics in colored potatoes that can help breeders to select genotypes for the generation of more colorful, healthy, and disease-resistant potatoes is one of the goals of this study.

Potatoes are indigenous in the Andes, having a single origin in the area of southern Peru and northwestern Bolivia, where they were domesticated approximately 7000–10,000 years ago (Spooner et al. 2005; Kiple and Ornelas 2000). About 5000 cultivated potato varieties exist worldwide (International Potato Center, <http://cipotato.org/potato/>), with the taxonomy being controversial with anywhere up to 20 species recognized (Takeda et al. 1988; Mateus et al. 2002). The major species grown worldwide is *Solanum tuberosum* L. (autotetraploid with 48 chromosomes), which we therefore have chosen for our investigations. Pigmented potatoes of this species seem to feature a huge variability in anthocyanin content and composition, which may be based on genetic differences. Thus, they supply a suitable model for investigating the regulation of anthocyanin biosynthesis in potato. We made use of the huge collection of the IPK Genebank (GLKS) in Groß Luesewitz (<http://glks.ipk-gatersleben.de/home.php>) which comprises more than 6100 potato accessions in total and about 2620 anthocyanin containing accessions (about 660 cultivated and 1960 wild accessions). This collection and the advance in analytical approaches lay the foundations to elucidate the phytochemical diversity in the crop plant potato on a newly revised level.

Overall, the tuber coloration patterns are highly variable and colors of tuber peel and flesh tissues do not always match. Potatoes with colored flesh usually have identically colored skin, but colored skin does not implicate that the flesh is colored too (De Jong et al. 2003). The pigmentation ranges from partial to complete. Different degrees of pigmentation result in specific coloration patterns including spots, stripes and rings (Brown 2006). For anthocyanins described in potato a rough pattern is already verified. The tuber colors are fundamentally determined by the matching profiles of the six major naturally occurring anthocyanidins. Red potatoes contain mainly acylated pelargonidin derivatives such as pelargonidin 3-*p*-coumaroylrutinoside-5-glucoside (Naito et al. 1998; Rodriguez-Saona et al. 1998). In contrast, purple or blue potatoes contain mixed patterns of the 3-*p*-coumaroylrutinoside-5-glucosides of petunidin, malvidin and peonidin (Lewis et al. 1998).

However, the tissue specific anthocyanin composition and its relation to the overall polyphenol constitution in colored potato tubers have been investigated infrequently.

Here, we analyzed the anthocyanin and polyphenol profiles of 57 naturally colored red and blue/purple potato varieties for extracts from tuber flesh and peel, respectively. Based on observed variations in anthocyanin composition and concentration, both between flesh and peel as well as between the individual varieties, potato tuber tissues of 19 cultivars have been selected for further quantitative analysis by LC–MS/MRM. Hierarchical clustering of the quantitative data, obtained for 21 anthocyanins and 31 additional polyphenols, facilitated the identification of cultivars and in particular of tissues with the highest variance in anthocyanin composition, and therefore presumably with the biggest differences in the anthocyanins biosynthesis regulation. Additionally, correlation analysis determined associations between anthocyanins and other polyphenols. Possible functions and regulatory mechanisms of the observed relations are discussed together with their impact on future breeding approaches.

## Materials and methods

### Plant material, cultivation and harvest

Tubers of 57 colored potato cultivars were obtained from the IPK Genebank (GLKS) in Groß Luesewitz (<http://glks.ipk-gatersleben.de/home.php>) and are listed in Supplemental Table S1. Potato tubers were field grown according to best agricultural practice at two different locations: (1) for LC-UV/MS analysis in Gross Luesewitz at two vegetation periods (2013 and 2014), and (2) for multiple reaction monitoring (MRM) analysis in Gatersleben (2015). Tubers were harvested after five months at maturity and sample material was prepared immediately. Tuber flesh and peel were manually separated, shock frozen under liquid nitrogen and stored at  $-80\text{ }^{\circ}\text{C}$  until lyophilization in a freeze dryer. Subsequently, the sample material was ground using a batch grinder (Janke and Kunkel KG, IKA factory, Staufen im Breisgau, Germany) and stored at  $4\text{ }^{\circ}\text{C}$  until usage.

Within the potato material examined, offsprings from self-pollination of two varieties, namely “Violettfleischige” (offsprings A to C) and “Blue Marker” (offspring A and B), were included. Furthermore, we made use of progenies from the crossing “Violettfleischige x Blue Marker” (offspring A to D). In case of the offsprings from “Violettfleischige” and “Violettfleischige x Blue Marker”, one genotype each was cultivated at two vegetation periods (Supplemental Table S1, entries A1 in 2013 and entries A2 in 2014, respectively) in Gross Luesewitz. Thus, together

with the planting of all cultivars in 2015 at another location, the selection of this material offered the opportunity to evaluate temporal and environmental influences, as by the location and the year of cultivation, for closely related cultivars or even within one progeny.

### Extraction of anthocyanins and other polyphenols from potato tubers

All utilized solvents were obtained from Th. Geyer (Renningen, Germany) at LC–MS grade. For LC-UV/MS based metabolite profiling flesh and peel from three tubers per cultivar were pooled. Extracts were prepared from 100 mg of lyophilized ground material using two times 500  $\mu\text{l}$  of a mixture of 70% methanol with 2% formic acid. The samples were weighted into a 2 ml reaction tube and after addition of the extraction solvent the tubes were vortexed for 3 s, shaken for 30 min on a thermomixer at  $4\text{ }^{\circ}\text{C}$  and centrifuged for 10 min at  $4\text{ }^{\circ}\text{C}$  with 28,000 g. The supernatants were transferred to fresh reaction tubes. After repetition of this procedure both supernatants were combined. For each sample, two independent extracts were made to obtain two technical replicates for the LC-UV/MS profiling.

For preparation of samples applied to LC–MS/MRM analysis, six tubers were pooled randomized from two to five plants per cultivar. The extraction procedure was the same as described above but using non acidified 70% methanol as solvent. For each sample, three independent extracts were made, referred to as technical replicates.

### LC-UV/MS profiling

LC-UV/MS profiling was carried out using a combination of an ultra-performance liquid chromatography (UPLC) instrument (H-class, Waters, Milford, MA, USA) with photodiode array (PDA) detection coupled to an ultra-high resolution time of flight mass spectrometer (UHR-TOF-MS, maXis Impact, Bruker Daltonics, Bremen, Germany) for MS detection. After centrifugation of the extracts 3  $\mu\text{l}$  per sample were injected. LC separation was performed on a reverse phase (RP) Acquity UPLC<sup>®</sup> CSH Phenyl-Hexyl column (130  $\text{\AA}$ ,  $2.1 \times 100\text{ mm}$ ,  $1.7\text{ }\mu\text{m}$ , Waters) in combination with an Acquity UPLC<sup>®</sup> CSH Phenyl-Hexyl VanGuard pre-column (130  $\text{\AA}$ ,  $2.1 \times 5\text{ mm}$ ,  $1.7\text{ }\mu\text{m}$ , Waters) according to the following protocol: from 98 to 90% of A for the first 3 min, from 90 to 80% A from 3 to 7 min, from 80 to 2% A from 7 to 10 min, and an isocratic hold for 3 min to clean the column. Solvent B was acetonitrile (Chemsolute, Renningen, Germany)/0.5% (v/v) formic acid and solvent A was 18 m $\Omega$  water (Merck, Darmstadt, Germany)/0.5% (v/v) formic acid. The temperature of the column was maintained at  $35\text{ }^{\circ}\text{C}$ . The

solvent was administered at a flow rate of 500  $\mu\text{l}/\text{min}$ . UV detection was performed in the range from 210 nm to 800 nm and UV chromatograms have been visually inspected at a wavelength of 515 nm for abundance of anthocyanins. For MS detection, the outlet of the PDA detector was coupled to the electrospray ionization (ESI) source (positive ion mode at 220 °C dry temperature, four bar nebulizer, 4000 V capillary voltage and a dry gas flow of 11 l/min) of the UHR-TOF-MS instrument using a splitter directing 83% of the eluate into the source. The instrument settings of the mass spectrometer were as follows: the mass range was set to  $m/z$  50–1500, with a hexapole radio frequency (RF) voltage of 100 V peak-to-peak (Vpp), a collision energy of 8 V, a funnel 1 RF of 300 Vpp, a funnel 2 RF of 600 Vpp, a prepulse storage time of 15  $\mu\text{s}$ , a transfer time of 50  $\mu\text{s}$  and a collision cell RF of 500 Vpp.

LC-UV/MS data were analyzed first using Bruker Compass DataAnalysis version 4.1 software for detection of molecular features. Resulting retention time (RT)/mass pairs were then used for extraction of ion chromatograms and integration of peak areas by means of QuantAnalysis 2.1 software (Bruker Daltonics). For principal component analysis (PCA), the module implemented in the Bruker Compass ProfileAnalysis 2.1 software (Bruker Daltonics) was utilized. The annotation of detected compounds is based on the comparison of the measured retention times and molecular ion masses with the literature data and metabolite data bases, such as KEGG, PubChem, ChemSpider, and Metlin (Supplemental Fig. S1g).

### LC-MS/MRM profiling

Metabolite profiling by means of LC separation coupled to triple quadrupole mass spectrometric (TQMS) detection was carried out using an Acquity UPLC system (Waters) coupled to a Xevo TQMS System (Waters). Directly prior injection the extracts were filtered (Millex-GV syringe filter unit, 0.22  $\mu\text{m}$ , PVDF, 33 mm, Millipore, Darmstadt, Germany). For each of the three extracts per sample, 2  $\mu\text{l}$  were injected twice and these six replicates per sample were measured in a randomized order. All utilized solvents were obtained from Sigma-Aldrich (Milano, Italy) at LC-MS grade.

Anthocyanins were separated on a RP Acquity UPLC<sup>®</sup> BEH C18 column (130  $\text{\AA}$ , 2.1  $\times$  150 mm, 1.7  $\mu\text{m}$ , waters), protected with an Acquity UPLC<sup>®</sup> BEH C18 pre-column (130  $\text{\AA}$ , 2.1  $\times$  5 mm, 1.7  $\mu\text{m}$ , waters). The following multistep linear gradient was used: from 95 to 60% of A for the first 4 min, from 60 to 45% A from 4 to 9 min, from 45 to 5% A from 9 to 11 min, and an isocratic hold for 3 min. Solvent B was methanol/5% (v/v) formic acid and solvent A was 18 m $\Omega$  water/5% (v/v) formic acid, administered at

a flow rate of 300  $\mu\text{l}/\text{min}$ . The column temperature was 40 °C. ESI was implemented in positive mode at 150 °C source temperature, 500 V capillary voltage, a desolvation gas flow of 1000 l/h and a desolvation temperature of 500 °C. Anthocyanin annotation is based on the literature data (Table 2) and entries of metabolite databases (KEGG, PubChem, ChemSpider, Metlin).

The separation of other polyphenols was performed with an Acquity UPLC<sup>®</sup> HSST3 column (100  $\text{\AA}$ , 2.1  $\times$  100 mm, 1.8  $\mu\text{m}$ , Waters) in combination with an Acquity UPLC<sup>®</sup> HSST3 pre-column (100  $\text{\AA}$ , 2.1  $\times$  5 mm, 1.8  $\mu\text{m}$ , waters). The solvent was administered at a flow rate of 400  $\mu\text{l}/\text{min}$ , according to the following protocol: from 95 to 80% of A for the first 4.5 min, from 80 to 55% A from 4.5 to 9 min, from 55 to 0% A from 9 to 11 min, and an isocratic hold for 3 min. Solvent B was acetonitrile/0.1% (v/v) formic acid and solvent A was 18 m $\Omega$  water/0.1% (v/v) formic acid. The temperature of the column was maintained at 40 °C. For ESI the capillary voltage was 3.5 kV in positive mode and  $-2.5$  kV in negative mode (Vrhovsek et al. 2012). The source was kept at 150 °C, desolvation temperature was 500 °C, cone gas flow was 50 l/h and desolvation gas flow was 800 l/h. For the annotation of potato polyphenols (P1-P31) listed in Table 3, the MRM measurement method was created on the basis of commercially available reference substances, referring to Vrhovsek et al. (2012). For each compound, two independent and orthogonal measures (retention time and two MRM transitions) relative to an authentic compound analyzed under identical experimental conditions have been considered. Thus, all the annotations belong to the level 1, non-novel metabolite identification.

Unit resolution was applied to each quadrupole. Respective MRM settings are listed in Tables 2 and 3. MRM data analysis was conducted using MassLynx 4.1 and TargetLynx software (Waters, Eschborn, Germany).

### Data analysis and visualization

Statistical analysis was performed with R software (R Core Team 2016) and visualized using package gplots (Warnes et al. 2015). Hierarchical clustering (Euclidean distance and complete linkage method) of log10 transformed phenolic metabolite intensities obtained from MRM peak areas was conducted to allow better comparison of large and small values. A dendrogram combined with a heat map depict the clustering results. Rows of the heat map represent tuber tissue samples of different cultivars, and columns represent the individual phenolic metabolites. Additionally, Pearson correlation analysis has been performed between the phenolic metabolite intensities of the cultivars, based on the integrated peak areas of the MRM analyses. Resulting correlation coefficients are visualized

either in a heat map representation, in a value matrix, or in scatter plots including regression lines. The significance is denoted by *P* value categories \*\*\* *P* < 0.001, \*\* *P* < 0.01, \* *P* < 0.05, · *P* < 0.1. Furthermore, the VANTED framework [Visualization and Analysis of Networks containing Experimental Data (Rohn et al. 2012)] was used to generate the anthocyanin biosynthesis pathway in potato tuber.

## Results

### LC-UV/MS analysis revealed tissue and cultivar specific patterns of polyphenols

To identify potato cultivars with high variation in their polyphenol patterns a sequential screening of tuber tissues of a large set of colored varieties was conducted. The workflow for metabolite profiling is shown in Fig. 1. First, 57 potato varieties differing in their tuber coloration have been evaluated for their polyphenol profiles by LC-UV/MS analysis. Thereby tuber flesh and peel were analyzed separately (57 colored potato cultivars, flesh and peel, Supplemental Table S1). Most pronounced differences were variations in anthocyanin composition and concentration, both between flesh and peel as well as between the individual varieties. One such example is shown in Fig. 2 for the varieties “Violettfleischige x Blue Marker-B” (#2), and “Rote Emmalie” (#49), which differ in the profile and the content of the main anthocyanins absorbing at 515 nm. However, to elucidate the main discriminating features of all acquired polyphenols we visualized the LC-MS dataset by principal component analysis (PCA).

Analyzing the main components of flesh and peel of the 57 potato cultivars in a projection of the data in two-dimensional space permits an overview of the patterns in the data (Fig. 3). With this method, it is possible to visualize whether these patterns are associated with tissue color, tissue type or variety. The PCA was performed on the complex data matrix of all measured polyphenols containing all the features (intensities of retention time-mass pairs) significantly detected across all samples. Figure 3a shows the scores plot of the first two components which allows for grouping of both tissue and color. PC1 separates the flesh and the peel samples with an explained variance of 48.2% and the different colored samples are separated on PC2 with 16.9% of explained variance. At PC2 three groups of samples were separated, namely the red, yellow, and blue/purple colored samples. That way a clustering of the samples in five main groups was obtained: (1) blue/purple flesh, (2) blue/purple peel, (3) red flesh, (4) red peel, and (5) yellow flesh. The variables related to the two components are shown in the loadings plot in Fig. 3b. For PC2 these variables mainly represent the color pigments,

especially the anthocyanins, while the variables for PC1 are represented by other phenolic compounds. The anthocyanins, the compounds we focused on that are mainly responsible for the separation of the differentially colored samples on PC2 are highlighted in the appropriate color. Anthocyanins that are responsible for blue to purple coloration of potato tuber tissues are mainly petunidin 3-*p*-coumaroylrutinoside-5-glucoside (6.09 min, 933.27 *m/z*), petunidin 3-feruloylrutinoside-5-glucoside (6.27 min, 963.27 *m/z*), and malvidin 3-*p*-coumaroylrutinoside-5-glucoside (6.69, 947.26 *m/z*). Responsible for the red coloration are mainly pelargonidin 3-feruloylrutinoside-5-glucoside (6.58 min, 917.27 *m/z*), pelargonidin 3-rutinoside (4.24 min, 579.17 *m/z*), pelargonidin 3-rutinoside-5-glucoside (3.57 min, 741.22 *m/z*) and pelargonidin 3-*p*-coumaroylrutinoside-5-glucoside (6.42 min, 887.26 *m/z*).

### Selection of most contrasting genotypes for quantitative LC-MS/MRM profiling

For further phytochemical characterization of the colored potato cultivars we focused on most abundant differences in anthocyanin profiles. The profiles mainly differ in anthocyanin composition and intensity. We assembled the 114 samples (flesh and peel of 57 colored potato cultivars) by grouping them for similar anthocyanin composition based on UV-absorption at 515 nm and MS profiles. Together, 24 distinct anthocyanin profiles (referred to as groups) were found across both analyzed tissues of all lines, each consisting of a number of red or blue/purple varieties (Supplemental Fig. S1 a-f). In tuber flesh, six different anthocyanin profile groups were observed, five of

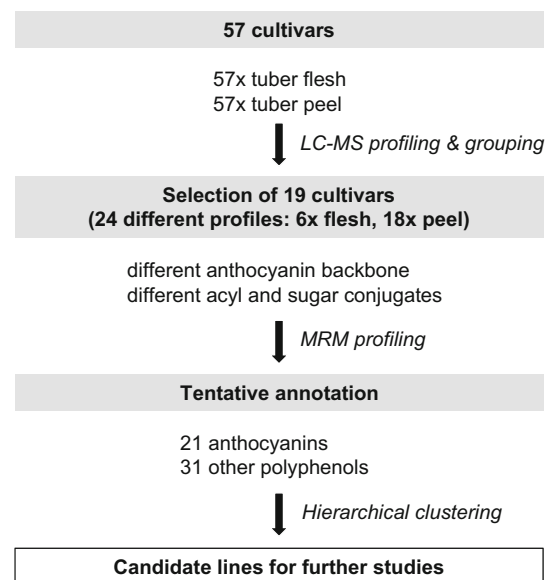


**Fig. 1** Schematic overview of the work flow for the metabolite screening of colored potato genotypes

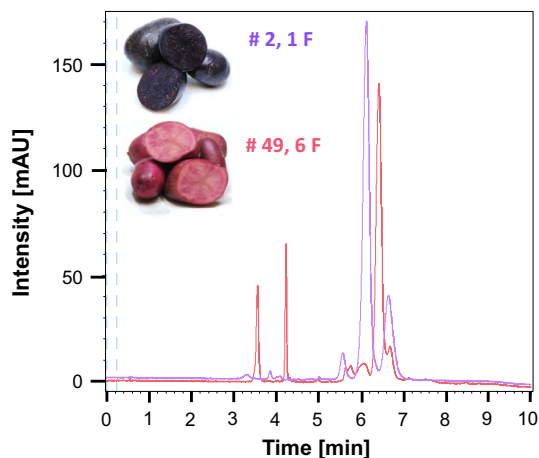


**Fig. 2** Overlay of contrasting anthocyanin profiles of *two colored* potato genotypes, analyzed by LC-UV/MS. UV-chromatograms at 515 nm; *purple flesh* (group 1 F) of variety “Violettefleischige x Blue Marker-B” (# 2), *red flesh* (group 6 F) of variety “Rote Emmalie” (# 49). Please also refer to Table 1 for anthocyanin profile groups (1 F and 6 F)

them relating to blue/purple tissue and one group observed in red-fleshed lines. For tuber peel, eighteen anthocyanin profile groups were assigned comprising six groups derived from red and 12 from blue/purple peel material (Table 1).

Most obvious variations between tissues and cultivars comprised the accumulation of anthocyanins with different backbones and different acyl and sugar conjugates. Red-fleshed potatoes mainly contain acylated pelargonidin derivatives (pelargonidin 3-*p*-coumaroylrutinoside-5-glucoside *m/z* 887.26 and pelargonidin 3-feruloylrutinoside-5-glucoside *m/z* 917.27), while blue/purple-fleshed lines harbor mixtures of several acylated derivatives of petunidin (petunidin 3-*p*-coumaroylrutinoside-5-glucoside *m/z* 933.26), peonidin (peonidin 3-*p*-coumaroylrutinoside-5-glucoside *m/z* 917.25), and malvidin (malvidin 3-*p*-coumaroylrutinoside-5-glucoside *m/z* 947.28). These data

were later validated by LC-MS/MS analysis and agree with previous studies by Lewis et al. (1998), Naito et al. (1998), and Rodriguez-Saona et al. (1998). Generally, higher absolute amounts and higher variability of anthocyanins were detected in potato peel. Thus, we kept tuber peel in our studies, although tuber flesh has the higher nutritional impact.

After grouping of all measured tissues according to their anthocyanin profiles, those cultivars showing the highest intensity of the main anthocyanins within each group were selected for further studies (Table 1 and Supplemental Fig. S2). In that way, 19 pigmented potato cultivars with different anthocyanin profiles in flesh (6 groups) and peel (18 groups) were selected, leading to an assortment of 24 samples of potato tuber tissue with various anthocyanin compositions, for the quantitative LC-MS/MS profiling.

### Compound annotation and selection of indicative molecular ions for LC-MS/MS analysis

The data obtained from the initial LC-UV/MS based anthocyanin profiling provide a strong case for description of phenotypic differences among colored potatoes. However, they lack identification and detection of differing peaks, especially for compounds with equal mass-to-charge ratios, and thus do not allow for quantification of related molecular ions. To fill this knowledge gap, we focused on the metabolite phenotyping of selected colored potato varieties by LC-MS/MS analysis of anthocyanin profiles and profiles for other polyphenolic substances. MRM provides a high level of selectivity for targeting these compounds and enables multiplexed, sensitive metabolite profiling. To ensure selective analysis of targeted compounds, a characteristic precursor ion eluting at a specific retention time (the so-called identifier) has to be defined together with a fragment ion (quantifier) preferentially produced during induced decay of the identifier molecular

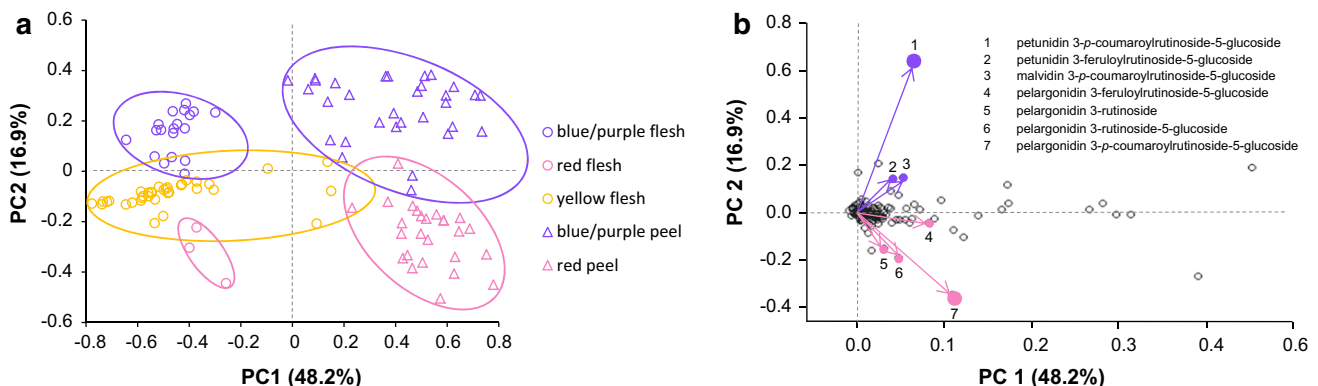


**Fig. 3** Results from principal component analysis of 114 samples obtained from tuber flesh and peel of 57 potato cultivars, presented as score (a) and loading (b) plots. Projection and related variable are

shown for PC1 and PC2. In the loadings plot, the anthocyanins mainly contributing to the variance between *red* and *blue/purple* tissue for PC2 are highlighted in the appropriate color

**Table 1** 19 selected colored potato cultivars, out of a total of 57 (Supplemental Table S1), analyzed by LC–MS/MS to assess polyphenol composition quantitatively

#	Name	Color		Group	
		Flesh	Peel	Flesh (6)	Peel (18)
2	Violettfleischige x Blue Marker-B	Purple	Purple	1 F	1 P
3	(Violettfleischige)-A1	Purple	Purple	3 F	2 P
6	(Blue Marker)-B	Purple	Purple		3 P
8	Blaue Ajanhuiri	Purple	Purple	5 F	4 P
9	Bangladesh	Yellow	Red		14 P
16	Königspurpur	Red	Red		15 P
17	Desiree	Yellow	Red		17 P
19	Early Rose	Yellow	Red		18 P
21	Shetland Blau I	Yellow	Purple		6 P
23	Rosamunda	White	Red		7 P
25	Weinberger Blaue	White	Purple		8 P
28	Mrs. Moerle's Purple Baker	White	Purple		5 P
39	Vogtländische Blaue	White	Purple		11 P
41	Purple	Purple	Purple		9 P
49	Rote Emmalie	Red	Red	6 F	
53	Violettfleischige x Blue Marker-D	Purple	Purple	2 F	10 P
54	(Violettfleischige)-A2	Purple	Purple		12 P
56	Rosemarie	Red	Red		16 P
57	Vitelotte	Purple	Purple	4 F	13 P

ion. Those values are then used to generate a MS method which sequentially acquires the compound specific data. To capture the anthocyanins and polyphenols in our extracts most comprehensively, we screened available literature data and compared retention orders and molecular ion signals with our available dataset from LC–UV/MS analysis. Those figures matching with values in our dataset were then used to tune respective MRM conditions and to generate MS methods for the analysis of anthocyanins and other polyphenols. In total, we generated MRM methods enabling the fragmentation-based quantification of 21 anthocyanins and 31 other polyphenols. Respective MRM settings for the assigned compounds are listed in Tables 2 and Table 3.

#### MRM data validated tissue and cultivar specific polyphenol patterns and indicated particular correlation of anthocyanins with other polyphenols

Material representative of the 24 anthocyanin profile groups (tuber flesh and peel of 19 selected potato cultivars, Table 1) has been measured by means of LC–MS/MS method. The generated data set was evaluated for differences in anthocyanin and other polyphenol profiles and abundance in these pigments.

The applied two-way hierarchical clustering, shown in Fig. 4, resulted in a dendrogram that displays the hierarchical relationship between the metabolite profiles of the

potato genotypes in addition to a heat map (Smoliński et al. 2002) which visualizes the log<sub>10</sub> scaled metabolite intensities of compound peak areas using a color scale from white (low value) to dark green (high value). Only compounds with at least five values with peak areas above the threshold of 10<sup>3</sup> across the different potato genotypes have been considered in the calculations (omitted compounds: P16, P19, P23, P24, and P31). The measured compounds are differently labeled in red (anthocyanins, A) and black (additional polyphenols, P).

Hierarchical clustering first revealed a separation of red and blue/purple tissue (horizontal axis). Main anthocyanins detected in red tissue are pelargonidin 3-*p*-coumaroylrutinoside-5-glucoside (A14), pelargonidin 3-feruloylrutinoside-5-glucoside (A17), and pelargonidin 3-rutinoside-5-glucoside (A2), while in blue/purple tissue the main anthocyanins are petunidin 3-*p*-coumaroylrutinoside-5-glucoside (A12) and malvidin 3-feruloylrutinoside-5-glucoside (A19), where the latter is more abundant in blue/purple tuber peel than in flesh. In addition, there is an obvious clustering of the type of tissue into peel and flesh, which mainly relates to other polyphenols that are present in tuber peel but could not be detected in flesh, such as coniferyl aldehyde (P26), 1,5-dicaffeoylquinic acid (P22), and daphnetin (P7), or compounds which were detected in peel in significantly higher amounts than in flesh-like vanillic acid (P9), ferulic acid (P17), vanillin (P14), and scopoletin (P18), among others. The content of those

**Table 2** MRM conditions for the quantitative analysis of potato anthocyanins

#	Tentative annotation	RT (min)	Transitions ( <i>m/z</i> )*	Cone (V)	Collision energy (eV)	Literature (references)
A1	Petunidin 3-rutinoside-5-glucoside	2.99	787 → <b>317</b> /625/ 479	20/20/ 40	40/20/40	a
A2	Pelargonidin 3-rutinoside-5-glucoside	3.20	741 → <b>271</b> /433/ 579	20/20/ 40	40/40/40	b, c
A3	Peonidin 3-rutinoside-5-glucoside	3.33	771 → <b>301</b> /463/ 609	20/20/ 40	40/20/40	b
A4	Malvidin 3-rutinoside-5-glucoside	3.42	801 → <b>331</b> /493/ 639	40/40/ 40	40/40/40	a
A5	Petunidin 3-rutinoside	3.98	625 → <b>317</b> /479	20/20	40/20	a
A6	Pelargonidin 3-rutinoside	4.16	579 → <b>271</b> /433	20/30	20/20	b, c
A7	Malvidin 3-rutinoside	4.40	639 → <b>331</b> /493	20/20	40/20	a
A8	Petunidin 3-caffeoylrutinoside-5-glucoside	4.41	949 → <b>317</b> /479/ 787	20/20/ 40	40/20/40	a
A9	Delphinidin 3- <i>p</i> -coumaroylrutinoside-5-glucoside	4.45	919 → <b>303</b> /465/ 757	20/20/ 40	40/20/40	a, c
A10	Pelargonidin feruloyl-xylosyl-glucosyl-galactoside	4.62	903 → <b>271</b>	20	40	d
A11	Cyanidin 3- <i>p</i> -coumaroylrutinoside-5-glucoside	4.74	903 → <b>287</b> /449	20/20	40/20	c, e
A12	Petunidin 3- <i>p</i> -coumaroylrutinoside-5-glucoside	4.78	933 → <b>317</b> /479/ 771	40/40/ 40	40/40/40	a, c
A13	Petunidin 3-feruloylrutinoside-5-glucoside	4.91	963 → <b>317</b> /479/ 801	30/40/ 20	20/40/20	a
A14	Pelargonidin 3- <i>p</i> -coumaroylrutinoside-5-glucoside	5.03	887 → <b>271</b> /433/ 725	20/40/ 40	40/40/40	a, b
A15	Peonidin 3- <i>p</i> -coumaroylrutinoside-5-glucoside	5.09	917 → <b>301</b> /463/ 755	30/40/ 40	20/40/40	a, b, c
A16	Malvidin 3- <i>p</i> -coumaroylrutinoside-5-glucoside	5.11	947 → <b>331</b> /493/ 785	30/20/ 40	20/20/40	a, c
A17	Pelargonidin 3-feruloylrutinoside-5-glucoside	5.14	917 → <b>271</b> /433/ 755	20/20/ 40	40/40/40	b
A18	Peonidin 3-feruloylrutinoside-5-glucoside	5.20	947 → <b>301</b> /463/ 785	20/40/ 40	40/40/40	a, b
A19	Malvidin 3-feruloylrutinoside-5-glucoside	5.21	977 → <b>331</b> /493/ 815	40/30/ 40	40/20/40	a
A20	Petunidin 3- <i>p</i> -coumaroylrutinoside	5.35	771 → <b>317</b> /479	20/40	40/40	a
A21	Pelargonidin 3- <i>p</i> -coumaroylrutinoside	5.67	725 → <b>271</b> /433	20/20	40/40	a, b

Quantitation ions are shown in bold (\*). All measurements were done in positive ion mode (ES+)

<sup>a</sup> Hillebrand et al. 2009

<sup>b</sup> Zhang et al. 2009

<sup>c</sup> [http://www.genome.jp/dbget-bin/www\\_bget?pathway+sot00942](http://www.genome.jp/dbget-bin/www_bget?pathway+sot00942)

<sup>d</sup> Kammerer et al. 2003

<sup>e</sup> Zubko et al. 1993

phenolic compounds, therefore, may be assumed as tissue specific.

Furthermore, the hierarchical clustering results indicate a correlation between anthocyanins and other polyphenols as there are compounds, such as kaempferol 3-rutinoside (P20), which is apparently color related because it is more abundant in red compared to blue/purple tuber tissue. The

same was found for blue/purple tuber tissue containing quercetin 3,4-rutinoside (P11) which was rarely detected in red tissue. For more detailed and corroborated assertions a correlation analysis was performed, providing the correlation coefficients and the *P* values for the evaluation of the significance of the detected correlations (Supplemental Fig. S3a-d).



**Table 3** MRM conditions for the quantitative analysis of potato polyphenols

#	Tentative annotation	RT (min)	Transitions ( <i>m/z</i> )*	Cone (V)	Collision energy (eV)	Polarity
P1	4-Aminobenzoic acid	2.17	137.95 → <b>76.98</b> /94.37	20/20	20/20	Positive
P2	Neochlorogenic acid	2.21	353.06 → <b>178.96</b> /191.00	26/26	18/18	Negative
P3	Chlorogenic acid	2.79	353.06 → <b>92.97</b> /191.00	36/36	38/20	Negative
P4	<i>p</i> -Hydroxybenzoic acid	2.88	138.87 → <b>64.90</b> /76.95	20/20	26/18	Positive
P5	Cryptochlorogenic acid	2.89	353.06 → <b>172.97</b> /178.96	34/34	14/16	Negative
P6	Fraxin	3.10	369.06 → <b>191.79</b> /206.94	32/32	32/20	Negative
P7	Daphnetin	3.20	178.93 → <b>104.96</b> /123.00	36/36	24/22	Positive
P8	Caffeic acid	3.23	180.95 → <b>117.01</b> /144.94	16/16	22/16	Positive
P9	Vanillic acid	3.29	168.95 → <b>64.98</b> /92.99	18/18	22/14	Positive
P10	2,4-Dihydroxy-benzoic acid	3.42	152.87 → <b>64.91</b> /109.00	24/24	16/14	Negative
P11	Quercetin 3,4-rutinoside	3.63	627.18 → <b>303.07</b> /465.08	18/18	32/16	Positive
P12	<i>p</i> -Coumaric acid	4.08	164.95 → <b>91.02</b> /119.03	16/16	24/26	Positive
P13	Coniferyl alcohol	4.09	163.03 → <b>103.03</b> /131.03	42716	18/10	Positive
P14	Vanillin	4.13	152.89 → <b>92.99</b> /124.98	20/20	16/10	Positive
P15	Rutin	4.22	611.25 → <b>303.00</b> /465.01	18/18	22/12	Positive
P16	Quercetin 3-glucoside	4.53	465.13 → <b>228.99</b> /303.01	18/18	48/12	Positive
P17	Ferulic acid	4.56	194.96 → <b>116.96</b> /144.97	42716	24/16	Positive
P18	Scopoletin	4.58	193.01 → <b>133.02</b> /161.08	14/14	16/10	Positive
P19	Sinapic acid	4.60	222.97 → <b>163.96</b> /207.97	30/30	18/14	Negative
P20	Kaempferol 3-rutinoside	5.05	595.19 → <b>287.00</b> /449.03	18/18	20/12	Positive
P21	Isorhamnetin 3-rutinoside	5.35	625.20 → <b>317.03</b> /479.04	18/18	20/12	Positive
P22	1,5-Dicaffeoylquinic acid	5.36	515.16 → <b>190.98</b> /353.06	26/26	28/16	Negative
P23	Kaempferol 3-glucoside	5.49	449.13 → <b>152.98</b> /287.01	16/16	48/14	Positive
P24	Quercetin 3-rhamnoside	5.59	449.13 → <b>129.03</b> /303.01	16/16	14/10	Positive
P25	Isorhamnetin 3-glucoside	5.63	479.14 → <b>302.02</b> /317.04	16/16	38/14	positive
P26	Coniferyl aldehyde	5.78	178.97 → <b>118.98</b> /146.99	22/22	18/14	Positive
P27	Dihydrokaempferol	6.13	289.03 → <b>152.99</b> /242.99	18/18	18/16	Positive
P28	Phlorizin	6.22	435.04 → <b>166.98</b> /273.03	32/32	30/16	Negative
P29	Luteolin	7.36	287.08 → <b>134.96</b> /152.99	52/52	30/32	Positive
P30	Cinnamic acid	7.61	149.00 → <b>103.00</b> /131.00	26/16	10/12	Positive
P31	Kaempferol	8.46	287.02 → <b>152.99</b> /164.97	50/50	32/26	Positive

Quantitation ions are shown in bold (\*)

### Significant correlations between polyphenols were detected

Linear relationships between metabolites have been evaluated by calculating the Pearson correlation coefficients. A number of compounds have not been included in the correlation analysis, namely A20, P10, P16, P19, P23, P24, P25, P31, because of very low (below  $10^3$ ) MRM acquired intensity values (Fig. 4, missing compounds and gray boxes). A condensed visualization of the Pearson correlation results is shown as a heat map in Fig. 5. Here, the correlation coefficients range from  $-1$  (negative correlation) to  $1$  (positive correlation), represented by the color key. Significant correlations are denoted by different

categories for *P* values. Related correlation coefficient  $|r|$ -values and significance *P* values are presented in Supplemental Fig. S3a, c, d. Additionally, scatter plots per interrelated compound pair were created visualizing the type of relationship between them (Supplemental Fig. S3a, b, c). A regression line depicts the linear association that is represented by Pearson correlation.

The most significant positive or negative correlations, as well as the least correlated metabolites are summarized in Table 4. Generally, positive associations were found with higher significance than negative ones. Of all calculated coherences the strongest and most significant one was found to be the positive correlation between the two anthocyanins delphinidin 3-*p*-coumaroylrutinoside-5-glucoside (A9) and

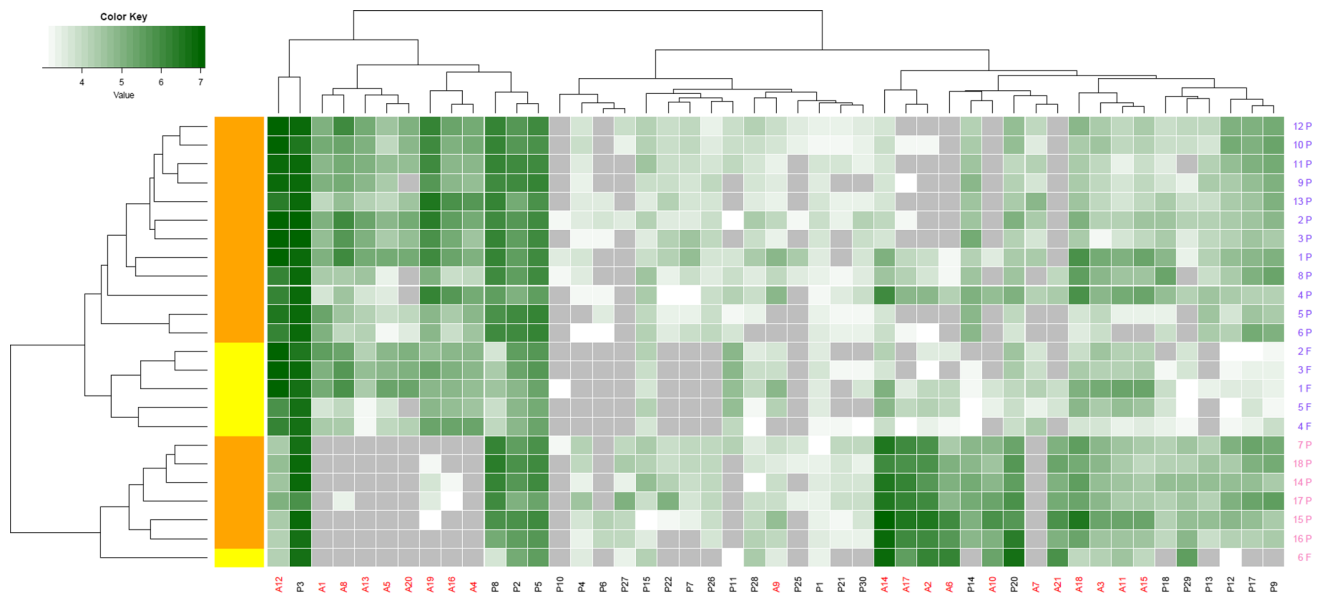


**Fig. 4** Two-way hierarchical clustering results visualized using a dendrogram combined with a heat map. The heat map represents the intensities (MRM peak areas, log<sub>10</sub> scaled values depicted in the color key [0; 7]) of the phenolic metabolites (*columns*) in the tuber tissues of the different cultivars (*rows*). On the horizontal axis, two main clusters represent cultivars with tuber colors *purple* and *red* and within each of the two clusters the two tissues flesh (*yellow bar*) and

peel (*orange bar*) cluster together. On the vertical axis, anthocyanins (A1 to A21, shown in *red*) and other polyphenols (P1 to P31, shown in *black*) form three main clusters indicative for their relative abundance in the different sample groups, and thus for their relationship. Abbreviations of cultivars and compounds are displayed according to Tables 1, 2, and 3, respectively. *Gray boxes* indicate peak areas below the threshold of 10<sup>3</sup>

peonidin 3-*p*-coumaroylrutinoside-5-glucoside (A15), with an *r*-value of 1 and a *P* value close to 0. Also, abundance of pelargonidin 3-rutinoside-5-glucoside (A2) positively correlates with the one of pelargonidin feruloyl-xylosyl-glucosyl-galactoside (A10), pelargonidin 3-*p*-coumaroylrutinoside-5-glucoside (A14), the main anthocyanin in red tuber tissue, and pelargonidin 3-*p*-coumaroylrutinoside (A21). Malvidin 3-rutinoside-5-glucoside (A4) was found significantly positive correlated with malvidin 3-*p*-coumaroylrutinoside-5-glucoside (A16). The strongest positive correlation between an anthocyanin and another polyphenol was calculated for pelargonidin 3-*p*-coumaroylrutinoside-5-glucoside (A14) and fraxin (P6). Other significant correlations were found for petunidin 3-caffeoylrutinoside-5-glucoside (A8) and phlorizin (P28), for pelargonidin 3-rutinoside (A6) with kaempferol 3-rutinoside (P20) and luteolin (P29), as well as for petunidin 3-feruloylrutinoside-5-glucoside (A13) with phlorizin (P28). Within the measured polyphenols 1,5-dicaffeoylquinic acid (P22) and dihydrokaempferol (P27) show the highest positive linkage. Also, kaempferol 3-rutinoside (P20) and luteolin (P29), *p*-hydroxybenzoic acid (P4) with 1,5-dicaffeoylquinic acid (P22) and dihydrokaempferol (P27), as well as vanillic acid (P9) and ferulic acid (P17) exhibit significant positive correlation of their abundance. The strongest and most significant negative correlation could be observed within the polyphenols for chlorogenic acid (P3), the main polyphenolic component in potato in general, and *p*-

hydroxybenzoic acid (P4) with an *r*-value of  $-0.77$  and a *P* value close to 0. Metabolites with no observed relationship were, for example, malvidin 3-rutinoside (A7) and cyanidin 3-*p*-coumaroylrutinoside-5-glucoside (A11), vanillin (P14) and scopoletin (P18), as well as pelargonidin 3-*p*-coumaroylrutinoside-5-glucoside (A14) and dihydrokaempferol (P27).

## Discussion

### Potato genotypes feature variable anthocyanin accumulation

The metabolite profiling of *Solanum tuberosum* genotypes revealed polyphenol patterns specific for particular tuber tissues and tuber coloration. In our analysis, two types of tuber tissue (flesh and peel) of red and blue/purple potato cultivars have been included. While certain polyphenols particularly allowed for the separation of peel and flesh tuber tissue, individual groups of anthocyanins were indicative for respective tissue coloration. Our comprehensive analysis of 57 pigmented *Solanum tuberosum* genotypes facilitated their grouping according to anthocyanin accumulation patterns, and thus possible genetic diversity regarding anthocyanin biosynthesis, for the first time.

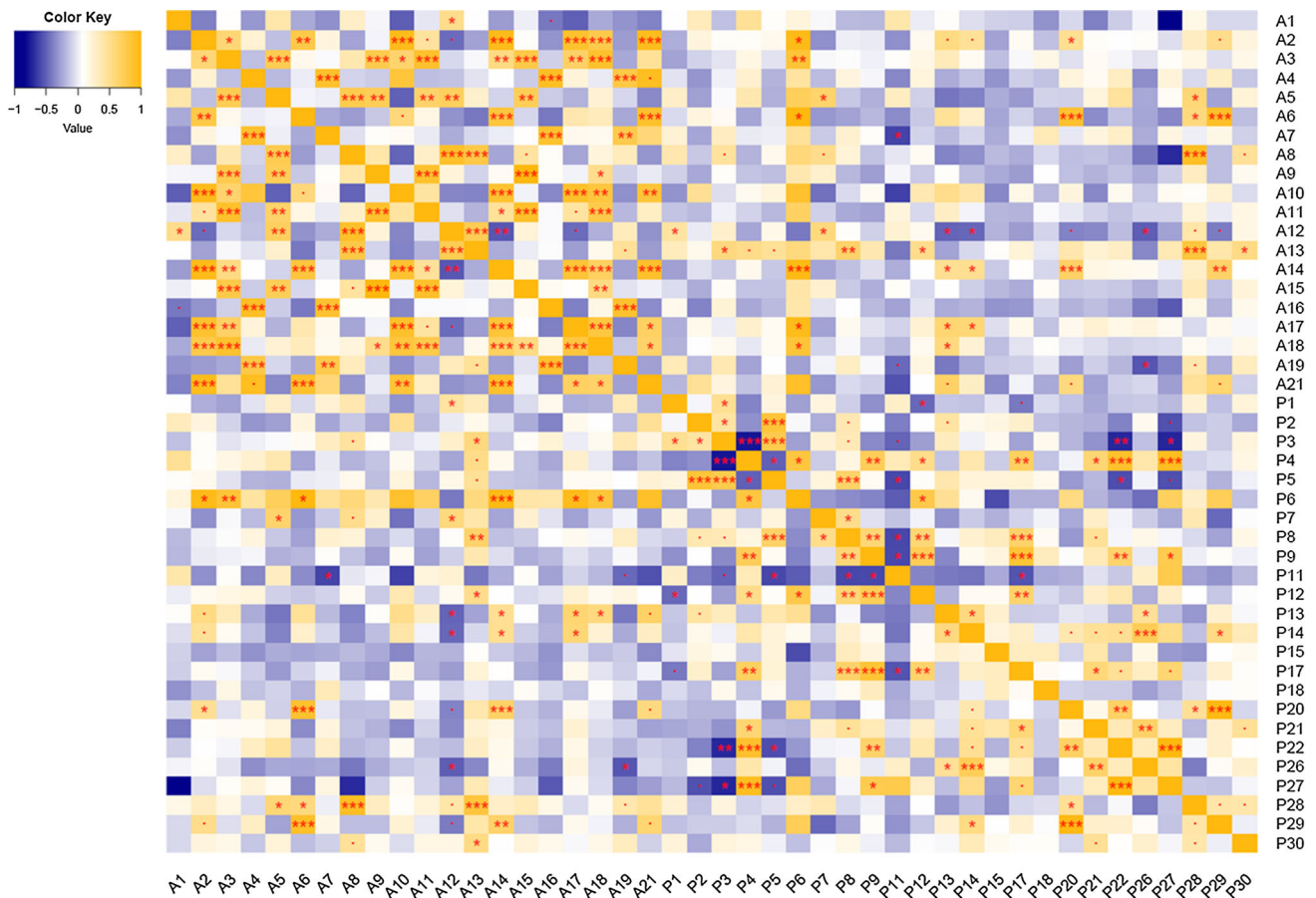


**Fig. 5** Pearson correlation analysis results depicted in a heat map. Correlation coefficient  $r$  is used to visualize the correlation between all anthocyanins (A1–A21) and additional polyphenolic compounds (P1–P31) detected in potato tuber tissues via LC–MS/MRM (color

key [–1; 1]). The significance is highlighted using categories for  $P$  values including \*\*\*  $P < 0.001$ , \*\*  $P < 0.01$ , \*  $P < 0.05$ , ·  $P < 0.1$ . Abbreviations of compounds are displayed according to Tables 2 and 3

We were able to tentatively annotate 27 individual anthocyanins in our data set, out of which 21 could be included in the quantitative MRM profiling of the 19 selected potato cultivars (Supplemental Fig. S1g). Our analysis revealed that red tuber tissue contains mainly pelargonidin derivatives, whereas blue/purple tuber tissue harbors mostly derivatives of malvidin and petunidin (Fig. 4; Table 4). These data confirm the findings of previous studies. In red potato tissue, pelargonidin 3-*p*-coumaroylrutinoside-5-glucoside (our compound A14) was identified as the main anthocyanin by Sachse (1973) already. Furthermore, acylated pelargonidin glycosides have been identified as main pigments in red potato tubers (Naito et al. 1998; Rodriguez-Saona et al. 1998). In blue/purple tissue, the main anthocyanin has been annotated as petunidin 3-*p*-coumaroylrutinoside-5-glucoside (our compound A12) by Andersen et al. (1991). In addition, malvidin and petunidin derivatives were described for blue-fleshed potatoes (Hillebrand et al. 2009). Conjugates of peonidin, as well as an

acylated delphinidin derivative, could be verified in both, red and blue/purple tuber tissue (Lachman and Hamouz 2005).

Notably, other than for the cultivar Vitelotte, polyphenolic profiles have not been described for any of the other genotypes included in our study. Also, few comparisons have been made between tuber flesh and peel. Compared with the literature data, in our study similar anthocyanin accumulation patterns were observed for red as well as for blue/purple tuber tissues. Additionally, we observed distinct anthocyanin profiles for peel of some genotypes, which together led to the categorization of several major genetic backgrounds for anthocyanin biosynthesis regulation in potato. Thus, we hypothesize at least four major groupings of potato cultivars based on anthocyanin accumulation, namely (1) no tuber coloration, (2) red tuber coloration, (3) blue/purple tuber coloration, and (4) particular peel coloration. Hence, the material assessed in our study provides a valuable resource to the selection of genotypes for the investigation of underlying regulatory

**Table 4** Examples for most significant positive or negative correlations and no observed correlations as obtained by means of Pearson correlation analysis (max. 5 examples per correlation type)

Type of correlation	Strongest positive correlation	Strongest negative correlation	No observed correlation
A vs. A	A9/A15 → +1.00***	A12/A14 → -0.53**	A7/A11 → 0.0018
	A2/A14 → +0.96***	A2/A12 → -0.46	A9/A10 → 0.0019
	A2/A10 → +0.95***	A12/A17 → -0.46	A4/A18 → 0.0035
	A2/A21 → +0.94***	A1/A16 → -0.41	A4/A6 → 0.0047
	A4/A16 → +0.91***		
A vs. P	A14/P6 → +0.97***	A7/P11 → -0.60*	A14/P27 → 0.00079
	A8/P28 → +0.91***	A19/P26 → -0.54*	A12/P2 → 0.001
	A6/P29 → +0.90***	A12/P26 → -0.51*	A17/P3 → 0.0014
	A6/P20 → +0.87***	A12/P13 → -0.49*	A2/P9 → 0.0014
	A13/P28 → +0.82***	A12/P14 → -0.47*	A11/P29 → 0.0029
P vs. P	P22/P27 → +0.98***	P3/P4 → -0.77***	P14/P18 → 0.0034
	P20/P29 → +0.97***	P3/P22 → -0.71**	P9/P26 → 0.0057
	P4/P27 → +0.93***	P3/P27 → -0.71*	P9/P28 → 0.0094
	P4/P22 → +0.88***	P5/P11 → -0.59*	
	P9/P17 → +0.84***	P8/P11 → -0.59*	

*P* values are represented by \*\*\*  $P < 0.001$ , \*\*  $P < 0.01$ , \*  $P < 0.05$ , ·  $P < 0.1$ . A anthocyanins; P other polyphenols. Abbreviations of compounds are displayed according to Table 2 and 3, respectively

mechanisms of anthocyanin biosynthesis and new breeding approaches.

Apart from pelargonidin feruloyl-xylosyl-glucosyl-galactoside (our compound A10), all other anthocyanins detected in our study have been described for potato previously (Hillebrand et al. 2009; Zhang et al. 2009; Zubko et al. 1993). Pelargonidin feruloyl-xylosyl-glucosyl-galactoside with *m/z* 903 (A10, Table 2) was identified earlier in black carrots (*Daucus carota* L. ssp. *sativus* var. *atrorubens* Alef.) by means of LC–MS/MS analysis (Kammerer et al. 2003; Algarra et al. 2014), but to our knowledge, it was detected for the first time in *Solanum tuberosum* in this study. We mainly detected this pelargonidin derivative in red potato tuber tissue, while only very small amounts were found in some of the blue/purple tubers. It is tempting to speculate about coherence between potato tuber and carrot anthocyanins. Both are tuberous roots and as such they are belowground organs growing in the dark. Although the role of anthocyanins in belowground organs is not clear yet, it is conceivable that they fulfill different functions compared to anthocyanins in light exposed plant tissues. Anthocyanins in fruits and flowers, for example, lead to a positive signaling to frugivores and pollinators due to their attracting color (Willson and Whelan 1990; Janson 1983). Accumulation of these pigments in young leaves is conducive to photoprotection (Liakopoulos et al. 2006). In underground organs, by contrast, the color aspect and the photo protective function are immaterial. In reproductive or storage tissues, such as potato tubers and tuberous carrot roots, anthocyanins are likely to have protective function against

pathogens and herbivores (Wegener and Jansen 2007; Innocenzi et al. 2004; Wang et al. 1997). They are associated with an improvement of preservation and thus lead to a reproductive advantage (Mano et al. 2007). This suggests that anthocyanin composition and regulation varies according to biological function and localization (Kovinich et al. 2014). The isolation of a regulatory MYB (*IbMYB1*) gene from purple-fleshed sweet potato which controls anthocyanin biosynthesis specifically in tuberous roots further approved this assumption (Mano et al. 2007).

Based on the literature sources and the KEGG database, we tentatively annotated compound A11 with *m/z* 903 (Table 2) as a cyanidin derivative (*m/z* 287), glycosylated with glucose (*m/z* 180) and rutinose (*m/z* 326) and acylated with *p*-coumaric acid (*m/z* 164). This anthocyanin was only described for callus cell lines of potato yet (*Solanum tuberosum* L. cv. Zarevo) by Zubko et al. (1993).

However, as annotation of anthocyanins in our study is based on the literature data and entries of metabolite databases only, full structural elucidation of side chain modifications remains to be conducted for both aforementioned compounds (A10 and A11) in potato tubers.

#### Certain anthocyanins show tissue type specificity in some potato genotypes

Our analysis revealed petunidin 3-*p*-coumaroylrutinoside-5-glucoside (A12) and malvidin 3-feruloylrutinoside-5-glucoside (A19) as the main anthocyanins in blue/purple tuber tissue. Interestingly, the latter is more abundant in

tuber peel than in flesh. Similarly, malvidin 3-*p*-coumaroylrutinoside-5-glucoside (A16) has found to be more abundant in tuber peel of blue/purple genotypes. In general, a higher concentration of malvidin derivatives could be detected in tuber peel compared to flesh. This could be attributed to the antibacterial effect of malvidin as recently demonstrated for anthocyanin extracts from *Syzygium cumini* (L.) (Gopu et al. 2015). The malvidin found in the peel of *S. cumini* fruits interrupts the quorum sensing of *Klebsiella pneumoniae*, and therefore enables an early defense response. As many bacterial species use this intercellular signaling mechanism it is conceivable that such defense reactions can also occur on malvidin-rich peels of blue/purple potatoes.

Furthermore, the results of our MRM analysis suggest that the tissue specific accumulation of some anthocyanins may be cultivar specific as well (Fig. 4). This seems to be the case for petunidin 3-caffeoylrutinoside-5-glucoside (A8). Other than the red peel of cultivar “Desiree” (group 17 P), this compound could only be detected in blue/purple tuber tissue and is most abundant in tuber flesh and peel of the two genotypes “Violettfleischige x Blue Marker-B” (group 1 F and group 1 P) and “Violettfleischige-A” (group 3 F and group 2 P). In contrast, pelargonidin feruloyl-xylosyl-glucosyl-galactoside (P10) is only present in flesh and peel of red colored cultivars, except the blue/purple varieties “Violettfleischige x Blue Marker-B” (group 1 F and group 1 P) and “Blaue Ajanhuiri” (group 5 F and group 4 P), where it was also found in both tissues. The peel of variety “Königspurpur” (group 15 P), shows the highest abundance for derivatives of pelargonidin and peonidin, while the main aglycon in cultivar “Vitelotte” (group 4 F) was found to be malvidin. Interestingly, the overall highest amounts of all four measured malvidin derivatives were detected in the tuber tissue of this variety and confirm malvidin derivatives as major pigments of blue-fleshed potatoes (Hillebrand et al. 2009; Eichhorn and Winterhalter 2005). This is highlighting Vitelotte as suitable potato variety to study the regulation of malvidin biosynthesis. Conjugates of peonidin were found in blue/purple and red tissue, while in the latter it seems to be more common, except for genotypes “Violettfleischige x Blue Marker-B” (group 1 P), “Weinberger Blaue” (group 8 P), and “Blaue Ajanhuiri” (group 4 P). The same accumulation pattern was observed for the acylated cyanidin derivative cyanidin 3-*p*-coumaroylrutinoside-5-glucoside (A11).

Together, our results hint to a cultivar-specific regulation of the tissue abundance of particular anthocyanins. Thus, lines with diverse accumulation patterns for anthocyanins in peel and flesh tissue represent powerful models to study the genic background of these particularities (Chen and Coe Jr 1977; Xie et al. 2015; Pattanaik et al. 2010).

### Abundance of certain other potato polyphenols also correlates with tissue type and coloration

About one third of the 31 tentatively annotated polyphenols were detected in all samples regardless of the color or type of the tissue. As an example, high amounts were found for caffeic acid (our compound P8) and derived chlorogenic acid isomers (our compounds P2, P3, and P5), whereas low abundance was observed for quercetin derivatives (our compounds P15, P16, and P21) as well as cinnamic acid (our compound P30). In contrast, the remaining compounds show various specificities.

Besides a clear separation of red and blue/purple tissue, our data analysis revealed an obvious clustering of tissues, e.g., peel and flesh. This separation mainly involves compounds that were strongly present in tuber peel but could not or only rarely be detected in flesh, such as caffeic acid (P8), coniferyl alcohol (P13), coniferyl aldehyde (P26), vanillin (P14), vanillic acid (P9), ferulic acid (P17) and *p*-coumaric acid (P12). Therefore, a tissue specificity can be assumed for these phenolic compounds, which has been reported recently for caffeic acid (Wang et al. 2015), and which is supposed to be linked to a special function of these compounds in the peel of belowground plant organs. Previous studies of sweet potato storage root indicated that periderm caffeic acid content is subject to genetic and environmental influences. This compound showed inhibitory activity on the growth of four sweet potato pathogenic fungi and germination of proso millet seeds, suggesting that high periderm caffeic acid levels contribute to the storage root defense chemistry (Harrison et al. 2003). Also, caffeic acid serves as a substrate of the lignin precursor ferulic acid (Valiñas et al. 2015) which is likewise elevated in potato tuber peel, contrasting to tuber flesh. Lignin and suberin have been implicated in the non-race-specific resistance of potato tuber discs to *Phytophthora* and *Phoma* spp. (Ampomah and Friend 1988) and their synthesis in the outer layer of the tubers may serve as a defense response of the plant that can potentially slow down pathogen spread.

Our data additionally hint to an interrelation of tissue color and polyphenol content, as elucidated for the anthocyanins. Some of the polyphenols accumulated strongly in red tuber tissue, such as kaempferol (P31), dihydrokaempferol (P27), kaempferol 3-glucoside (P23), kaempferol 3-rutinoside (P20) and luteolin (P29), whereas others such as quercetin 3,4-rutinoside (P11) and quercetin 3-rhamnoside (P24) were found with higher content in blue/purple tissue. This observation is in accordance with the anthocyanin biosynthesis where kaempferol derivatives act as direct precursor for pelargonidins leading to red coloration while quercetin is the precursor used for the biosynthesis of cyanidins/peonidins and delphinidins/malvidins mainly

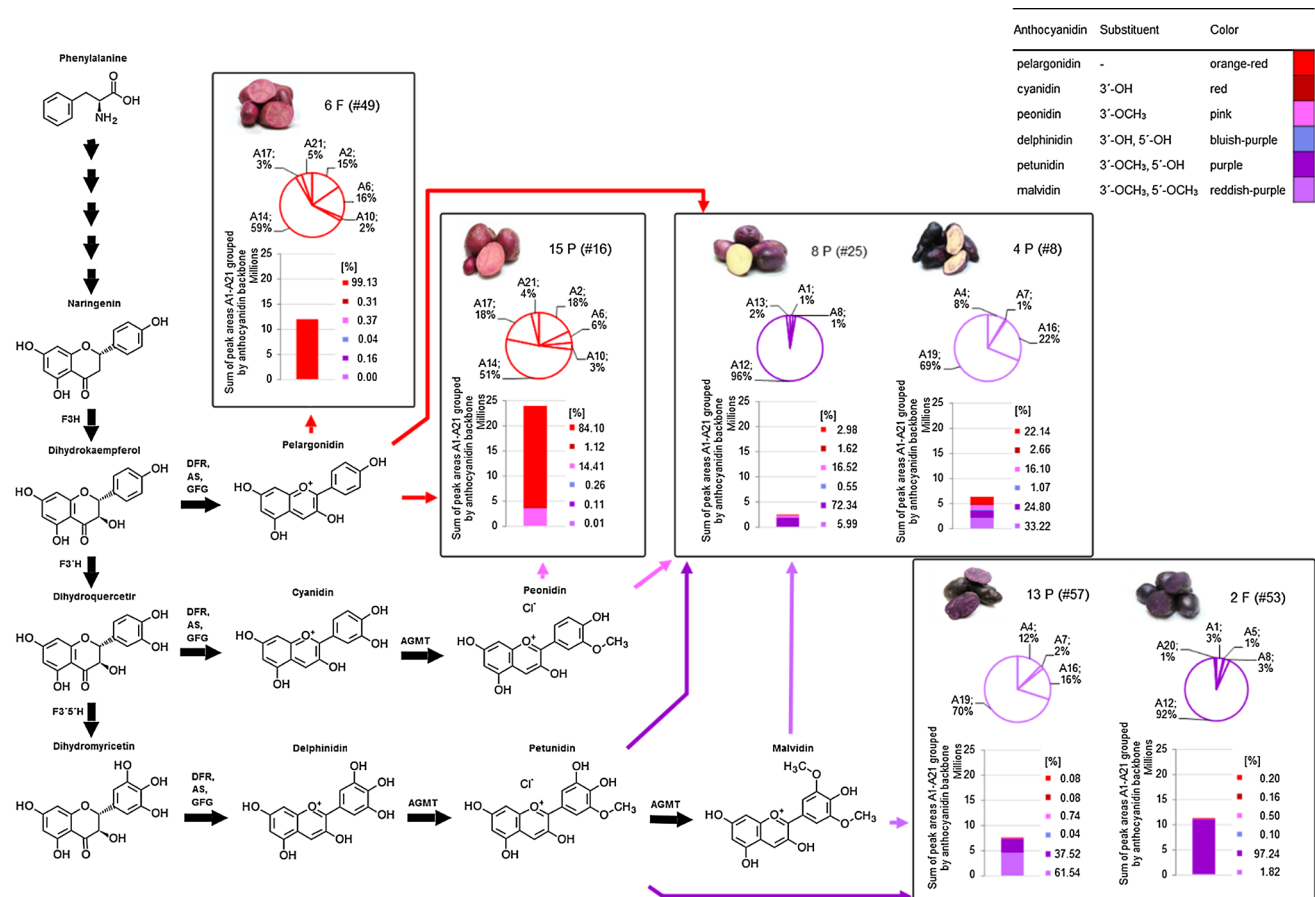


**Fig. 6** Schematic overview of the anthocyanidin biosynthesis pathway in potato tuber. Stacked bar charts are shown for selected candidate cultivars with representative anthocyanin profiles, where total anthocyanin content is presented as the sum of peak areas (compound A1–A21) and the relative amount of anthocyanidin derivatives is given. Additionally, the proportion of individual anthocyanins for the major aglycone of each candidate cultivar is visualized as a pie chart. Calculations are based on LC–MS/MS data of the 21 detected anthocyanins. Graphic elements (*columns, pie*

*charts, and arrows*) are stained according to the dominating color of the respective aglycone. *AGMT* anthocyanidin-glycoside-3-*O*-methyl transferase; *AS* anthocyanin synthase; *DFR* dihydroflavonol-4-reductase; *F3H* flavanone-3-hydroxylase; *F3'H* flavonoid-3'-hydroxylase; *F3'H* flavonoid-3,5'-hydroxylase; *GFG* UDP-glucose 3-*O*-flavonoid glucosyltransferase. Cultivars and abbreviations of compounds are displayed according to Tables 1 and 2, respectively [produced using VANTED (Rohn et al. 2012); structural formulas of metabolites are included from KEGG database (Kanehisa et al. 2015)]

leading to blue/purple pigmentation (Fig. 6, [http://www.genome.jp/kegg-bin/show\\_pathway?map00941](http://www.genome.jp/kegg-bin/show_pathway?map00941)).

Most pronounced was the association of kaempferol 3-rutinoside (P20) and luteolin (P29) with red tuber flesh tissue of variety “Rote Emmalie” (profile group 6 F). Generally, potato peel contains significantly higher concentrations of free and bound phenolics than the flesh (Nara et al. 2006). The flavonoid luteolin, for example, possesses a variety of pharmacological activities, including antioxidant, anti-inflammatory, antimicrobial and anticancer activities (Lopez-Lazaro 2009). The increased accumulation of luteolin in tuber flesh points to a particular nutritional importance of variety “Rote Emmalie”. Likewise, quercetin 3,4-rutinoside (P11) was found to be more abundant in blue/purple tuber flesh than in peel. Among the 31 polyphenols analyzed this compound is the only one

with higher abundance in blue/purple tuber flesh compared to tuber peel, and therefore assumed to contribute to the nutritional value of the blue/purple potatoes.

### Strongest metabolite correlations relate to particularities of flavonoid biosynthesis in pigmented tissues

Generally, higher anthocyanin accumulation in potato coincided with higher contents of total soluble phenols in pigmented potato varieties when compared with yellow flesh varieties (Wegener and Jansen 2007). Accordingly, we detected more positive than negative correlations in our data set. Whereas the detected positive correlations show similar strengths for anthocyanins, other polyphenols, and

anthocyanins with other polyphenols, negative correlations were found most significant within the group of other polyphenols and least significant within the anthocyanins.

Confirming and emphasizing our previous findings that red tuber tissue mainly contains pelargonidin 3-*p*-coumaroylrutinoside-5-glucoside (A14), whereas blue/purple tuber tissue mostly harbors petunidin 3-*p*-coumaroylrutinoside-5-glucoside (A12), these two compounds showed the most significant negative association.

As known from other studies (Andre et al. 2007; Friedman 1997) chlorogenic acid and its isomers (P3, P2, and P5) dominated the polyphenolic profile of each cultivar regardless of amount and composition of anthocyanins and other polyphenols. No correlation between chlorogenic acid and tissue type or color associated types of anthocyanins could be observed, as this compound was detected in all samples in similar amounts. Contrary, for conventional yellow-fleshed potato varieties it has been reported that chlorogenic acid is more abundant in potato peel compared to flesh (Wang et al. 2015). According to previous studies showing that potatoes with red or purple flesh have markedly higher amounts of chlorogenic acid and its derivatives (Andre et al. 2007; Payyavula et al. 2015; Navarre et al. 2011), which we could confirm by a positive correlation between chlorogenic acid content and the overall anthocyanin amount. The general correlation of anthocyanin and chlorogenic acid accumulation corroborates the assumption of mutual regulatory mechanisms for anthocyanin, polyphenol and phenolic acid biosynthesis, as shown in previous studies indicating synergistic effects (Mazzaracchio et al. 2004). This is in accordance with the role of chlorogenic acid as a central intermediate in phenylpropanoid biosynthesis (Payyavula et al. 2015; Valiñas et al. 2015).

Kaempferol 3-rutinoside (P20) and luteolin (P29) exhibit a high correlation not only among themselves, but also to four of the six pelargonidin derivatives analyzed. However, the reason for this strong connection of the biosynthesis of these two compounds remains unclear as no direct link has been reported so far, although both metabolites are products as well as intermediates of flavone and flavonol biosynthesis. We hypothesized a role of both compounds (P20 and P29) during regulation of biosynthesis of pelargonidins, probably by influencing the flow of precursors in this direction.

### Concluding remarks and perspectives

Here, we describe differential polyphenol patterns, particularly focusing on anthocyanins, of many pigmented potato cultivars for the first time. Our data allowed the assignment of potato genotypes to the appropriate position in the biosynthetic pathway according to their anthocyanin

profile, suggesting a dominant metabolic flow in particular branches of the flavonoid pathway (Fig. 6). Overall, diverse interactions in a highly complex network of enzymatic reactions can be inferred to be responsible for this diversity. Differently regulated hydroxylation and methylation events at the B-ring of dihydroflavonols lead to the formation of anthocyanidin backbones that are specific for either red or blue/purple tuber tissues (Fig. 6, bar charts). On the other hand, similar glycosylation and acylation reactions can be supposed at least for the main anthocyanidin precursors detected in red and blue/purple tissue (Fig. 6, pie charts). This leads to the assumption that besides the superior regulation of the expression and/or enzymatic activity of hydroxylases and methyltransferases, differently colored potato tissues presumably comprise more or less the same set of downstream glycosyl- and acyltransferases.

Being a key step in the biosynthesis of differentially colored anthocyanins, we postulate a significant difference in the regulation of flavonoid-3,5-hydroxylase, catalyzing the transformation of dihydroquercetin to dihydromyricetin, in blue/purple tuber tissue. This enzyme is regarded as the precursor for the synthesis of delphinidin, petunidin and malvidin in potato anthocyanin biosynthesis (Stushnoff et al. 2010). Thus, among others, flavonoid-3,5-hydroxylase will be the subject of our further research investigating the regulation of potato anthocyanin biosynthesis.

Besides, strong interactions of anthocyanin accumulation and abundance of other polyphenols motivated us to speculate about further regulatory elements of this biosynthesis pathway. In this regards, our genotype collection provides material of high value for the investigation of anthocyanin side chain regulation and tissue specific accumulation and function, in crops with belowground storage organs.

In our LC-UV/MS analysis, we have included a few genotypes grown at different growth periods. One such example is genotype #3 (grown in 2013) and its genetically identical tuber propagation genotype #54 (grown in 2014). We observed differing anthocyanin profiles for tuber peel of cultivars #3 and #54 (Supplemental Fig. S1), which are likely attributed to environmental changes during cultivation in 2013 and in 2014. To prove to which extent environmental conditions can influence anthocyanin patterns in colored potatoes will be the subject of future studies.

Additionally, our data imply that some anthocyanin profiles are more stable than others and maybe genotype or tissue specific. Prominent examples are the selfed lines of the cultivars “Violettfleischige” (accession GLKS 12066) and “Blue Marker” (accession GLKS 12477) and their crosses (accession GLKS 12066 x accession GLKS 12477). Potato flesh of the selfed lines showed one dominating

anthocyanin profile (profile group 2 F), while anthocyanin profiles of their peel samples strongly varied dependent on the genotype (profile groups 1 P, 2 P, 3 P, 10 P and 12 P, Supplemental Fig. S1). Thus, we postulate a potential dominance of some genotypes concerning these stable anthocyanin profiles, which constitutes an important aspect in breeding programs.

**Author contribution statement** AO, AM, SM and H-PM contributed to conception and design of this study and participated in drafting and revision of the manuscript. KD selected and provided plant material. AO cultivated the plants, conducted experiments, analyzed data, and wrote the manuscript. PA technically supported sample measurement. AH realized statistics and performed data visualization. All authors read and approved the manuscript.

**Acknowledgements** This research has been financially supported by the ERA-IB ANTHOPLUS project (031A336A0) and by the COST Action “The quest for tolerant varieties—Phenotyping at plant and cellular level” (FA1306).

## References

- Algarra M, Fernandes A, Mateus N, de Freitas V, da Silva JCE, Casado J (2014) Anthocyanin profile and antioxidant capacity of black carrots (*Daucus carota* L. ssp. *sativus* var. *atrorubens* Alef.) from Cuevas Bajas, Spain. *J Food Compos Anal* 33(1):71–76
- Ampomah YA, Friend J (1988) Insoluble phenolic compounds and resistance of potato tuber disc to *Phytophthora* and *Phoma*. *Phytochemistry* 27(8):2533–2541
- Andersen ØM, Opheim S, Aksnes DW, Frøystein NÅ (1991) Structure of petanin, an acylated anthocyanin isolated from *Solanum tuberosum*, using homo- and hetero-nuclear two-dimensional nuclear magnetic resonance techniques. *Phytochem Anal* 2(5):230–236
- Andre CM, Oufir M, Guignard C, Hoffmann L, Hausman J-F, Evers D, Larondelle Y (2007) Antioxidant profiling of native Andean potato tubers (*Solanum tuberosum* L.) reveals cultivars with high levels of  $\beta$ -carotene,  $\alpha$ -tocopherol, chlorogenic acid, and petanin. *J Agr Food Chem* 55(26):10839–10849
- Bagchi D, Sen C, Bagchi M, Atalay M (2004) Anti-angiogenic, antioxidant, and anti-carcinogenic properties of a novel anthocyanin-rich berry extract formula. *Biochemistry (Moscow)* 69(1):75–80
- Bridle P, Timberlake C (1997) Anthocyanins as natural food colours—selected aspects. *Food Chem* 58(1):103–109
- Brown C (2006) Anthocyanin and carotenoid contents in potato: breeding for the specialty market. *Proc Ida Winter Commod Sch* 39:157–163
- Butelli E, Titta L, Giorgio M, Mock H-P, Matros A, Peterek S, Schijlen EG, Hall RD, Bovy AG, Luo J (2008) Enrichment of tomato fruit with health-promoting anthocyanins by expression of select transcription factors. *Nat Biotechnol* 26(11):1301–1308
- Castaneda-Ovando A, de Lourdes Pacheco-Hernández M, Páez-Hernández ME, Rodríguez JA, Galán-Vidal CA (2009) Chemical studies of anthocyanins: a review. *Food Chem* 113(4):859–871
- Chalker-Scott L (1999) Environmental significance of anthocyanins in plant stress responses. *Photochem Photobiol* 70:1–9
- Chen S-M, Coe E Jr (1977) Control of anthocyanin synthesis by the C locus in maize. *Biochem Genet* 15(3–4):333–346
- De Jong W, De Jong D, De Jong H, Kalazich J, Bodis M (2003) An allele of dihydroflavonol 4-reductase associated with the ability to produce red anthocyanin pigments in potato (*Solanum tuberosum* L.). *Theor Appl Genet* 107(8):1375–1383
- Eichhorn S, Winterhalter P (2005) Anthocyanins from pigmented potato (*Solanum tuberosum* L.) varieties. *Food Res Int* 38(8):943–948
- Fournier-Level A, Huguency P, Verriès C, This P, Ageorges A (2011) Genetic mechanisms underlying the methylation level of anthocyanins in grape (*Vitis vinifera* L.). *BMC Plant Biol* 11(1):179
- Friedman M (1997) Chemistry, biochemistry, and dietary role of potato polyphenols. A review. *J Agr Food Chem* 45(5):1523–1540
- Gopu V, Kothandapani S, Shetty PH (2015) Quorum quenching activity of *Syzygium cumini* (L.) Skeels and its anthocyanin malvidin against *Klebsiella pneumoniae*. *Microb Pathog* 79:61–69
- Goto T, Kondo T, Tamura H, Imagawa H, Iino A, Takeda K (1982) Structure of gentiodelphin, an acylated anthocyanin isolated from *Gentiana makinoi*, that is stable in dilute aqueous solution. *Tetrahedron Lett* 23(36):3695–3698
- Harrison HF, Peterson JK, Snook ME, Bohac JR, Jackson DM (2003) Quantity and potential biological activity of caffeic acid in sweet potato [*Ipomoea batatas* (L.) Lam.] storage root periderm. *J Agr Food Chem* 51(10):2943–2948
- He J, Giusti MM (2010) Anthocyanins: natural colorants with health-promoting properties. *Annu Rev Food Sci Technol* 1:163–187
- Hillebrand S, Naumann H, Kitzinski N, Köhler N, Winterhalter P (2009) Isolation and characterization of anthocyanins from blue-fleshed potatoes (*Solanum tuberosum* L.). *Food 3*(1):96–101
- Innocenzi V, Arnone S, Lai A, Musmeci S, Gambino P (2004) Eliciting of resistance against potato tuber moth larvae in tubers of *Solanum tuberosum* (+) *S. pinnatisectum* hybrids. In: Meeting of the physiology section of the european association for potato research, vol 684, pp 135–142
- Janson CH (1983) Adaptation of fruit morphology to dispersal agents in a neotropical forest. *Science (Washington)* 219(4581):187–189
- Kammerer D, Carle R, Schieber A (2003) Detection of peonidin and pelargonidin glycosides in black carrots (*Daucus carota* ssp. *sativus* var. *atrorubens* Alef.) by high performance liquid chromatography/electrospray ionization mass spectrometry. *Rapid Commun Mass Spectrom* 17(21):2407–2412
- Kanehisa M, Sato Y, Kawashima M, Furumichi M, Tanabe M (2015) KEGG as a reference resource for gene and protein annotation. *Nucleic Acids Res*. doi:10.1093/nar/gkv1070
- Kim HW, Kim JB, Cho SM, Chung MN, Lee YM, Chu SM, Che JH, Kim SN, Kim SY, Cho YS (2012) Anthocyanin changes in the Korean purple-fleshed sweet potato, Shinzami, as affected by steaming and baking. *Food Chem* 130(4):966–972
- Kiple KF, Ornelas KC (2000) The Cambridge world history of food, vol 1. Cambridge University Press, Cambridge, pp 2000–2153
- Kovinich N, Kayanja G, Chanoca A, Riedl K, Otegui MS, Grotewold E (2014) Not all anthocyanins are born equal: distinct patterns induced by stress in *Arabidopsis*. *Planta* 240(5):931–940
- Lachman J, Hamouz K (2005) Red and purple coloured potatoes as a significant antioxidant source in human nutrition—a review. *Plant Soil Environ* 51(11):477
- Lewis CE, Walker JR, Lancaster JE, Sutton KH (1998) Determination of anthocyanins, flavonoids and phenolic acids in potatoes. I: Coloured cultivars of *Solanum tuberosum* L. *J Sci Food Agr* 77(1):45–57
- Liakopoulos G, Nikolopoulos D, Klouvatou A, Vekkos K-A, Manetas Y, Karabourniotis G (2006) The photoprotective role of



- epidermal anthocyanins and surface pubescence in young leaves of grapevine (*Vitis vinifera*). *Ann Bot-London* 98(1):257–265
- Lila MA (2004) Anthocyanins and human health: an in vitro investigative approach. *Biomed Res Int* 2004(5):306–313
- Lopez-Lazaro M (2009) Distribution and biological activities of the flavonoid luteolin. *Mini reviews in Med Chem* 9(1):31–59
- Mano H, Ogasawara F, Sato K, Higo H, Minobe Y (2007) Isolation of a regulatory gene of anthocyanin biosynthesis in tuberous roots of purple-fleshed sweet potato. *Plant Physiol* 143(3):1252–1268
- Mateus N, de Pascual-Teresa S, Rivas-Gonzalo JC, Santos-Buelga C, de Freitas V (2002) Structural diversity of anthocyanin-derived pigments in port wines. *Food Chem* 76(3):335–342
- Mazza G (2007) Anthocyanins and heart health. *Ann Ist Super Sanità* 43(4):369
- Mazzaracchio P, Pifferi P, Kindt M, Munyaneza A, Barbiroli G (2004) Interactions between anthocyanins and organic food molecules in model systems. *Int J Food Sci Technol* 39(1):53–59
- Naito K, Umemura Y, Mori M, Sumida T, Okada T, Takamatsu N, Okawa Y, Hayashi K, Saito N, Honda T (1998) Acylated pelargonidin glucosides from a red potato. *Phytochemistry* 47(1):109–112
- Nara K, Miyoshi T, Honma T, Koga H (2006) Antioxidative activity of bound-form phenolics in potato peel. *Biosci Biotech Bioch* 70(6):1489–1491
- Navarre DA, Pillai SS, Shakya R, Holden MJ (2011) HPLC profiling of phenolics in diverse potato genotypes. *Food Chem* 127(1):34–41
- Ohgami K, Ilieva I, Shiratori K, Koyama Y, Jin X-H, Yoshida K, Kase S, Kitaichi N, Suzuki Y, Tanaka T (2005) Anti-inflammatory effects of aronia extract on rat endotoxin-induced uveitis. *Invest Ophthalmol Vis Sci* 46(1):275–281
- Pattanaik S, Kong Q, Zaitlin D, Werkman JR, Xie CH, Patra B, Yuan L (2010) Isolation and functional characterization of a floral tissue-specific R2R3 MYB regulator from tobacco. *Planta* 231(5):1061–1076
- Payyavula RS, Shakya R, Sengoda VG, Munyaneza JE, Swamy P, Navarre DA (2015) Synthesis and regulation of chlorogenic acid in potato: rerouting phenylpropanoid flux in HQT-silenced lines. *Plant Biotech J* 13(4):551–564
- Prior RL (2003) Fruits and vegetables in the prevention of cellular oxidative damage. *Am J Clin Nutr* 78(3):570S–578S
- Rodriguez-Saona LE, Giusti MM, Wrolstad RE (1998) Anthocyanin pigment composition of red-fleshed potatoes. *J Food Sci* 63(3):458–465
- Rohn H, Junker A, Hartmann A, Grafahrend-Belau E, Treutler H, Klapperstück M, Czauderna T, Klukas C, Schreiber F (2012) VANTED v2: a framework for systems biology applications. *BMC Syst Biol* 6(1):1
- Sachse J (1973) Anthocyane in den Kartoffelsorten Urgenta und Desirée (*Solanum tuberosum* L.). *FOOD SCIENCE AND TECHNOLOGY-LEBENSMITTEL-WISSENSCHAFT & TECHNOLOGIE* 153(5):294–300
- Smoliński A, Walczak B, Einax J (2002) Hierarchical clustering extended with visual complements of environmental data set. *Chemometr Intell Lab* 64(1):45–54
- Spooner DM, McLean K, Ramsay G, Waugh R, Bryan GJ (2005) A single domestication for potato based on multilocus amplified fragment length polymorphism genotyping. *P Natl Acad Sci USA* 102(41):14694–14699
- Steyn W, Wand S, Holcroft D, Jacobs G (2002) Anthocyanins in vegetative tissues: a proposed unified function in photoprotection. *New Phytol* 155(3):349–361
- Stushnoff C, Ducreux LJ, Hancock RD, Hedley PE, Holm DG, McDougall GJ, McNicol JW, Morris J, Morris WL, Sungurtas JA (2010) Flavonoid profiling and transcriptome analysis reveals new gene–metabolite correlations in tubers of *Solanum tuberosum* L. *J Exp Bot* 61(4):1225–1238
- Takeda K, Kumegawa C, Harborne JB, Self R (1988) Pelargonidin 3-(6'-succinyl glucoside)-5-glucoside from pink *Centaurea cyanus* flowers. *Phytochemistry* 27(4):1228–1229
- Team RC (2016) R: a language and environment for statistical computing. R Foundation for Statistical Computing, Vienna, Austria. 2015. <http://www.R-project.org>
- Tsuda T (2016) Recent progress in anti-obesity and anti-diabetes effect of berries. *Antioxidants* 5(2):13
- Valiñas MA, Lanteri ML, ten Have A, Andreu AB (2015) Chlorogenic acid biosynthesis appears linked with suberin production in potato tuber (*Solanum tuberosum*). *J Agr Food Chem* 63(19):4902–4913
- Vrhovsek U, Masuero D, Gasperotti M, Franceschi P, Caputi L, Viola R, Mattivi F (2012) A versatile targeted metabolomics method for the rapid quantification of multiple classes of phenolics in fruits and beverages. *J Agr Food Chem* 60(36):8831–8840
- Wang H, Cao G, Prior RL (1997) Oxygen radical absorbing capacity of anthocyanins. *J Agr Food Chem* 45(2):304–309
- Wang Q, Cao Y, Zhou L, Jiang C-Z, Feng Y, Wei S (2015) Effects of postharvest curing treatment on flesh colour and phenolic metabolism in fresh-cut potato products. *Food Chem* 169:246–254
- Warnes G, Bolker B, Bonebakker L, Gentleman R, Liaw W, Lumley T (2015) Package “gplots”: various R programming tools for plotting data. R package version 3.0. 1. <https://cran.r-project.org/web/packages/gplots/gplots.pdf>
- Wegener CB, Jansen G (2007) Soft-rot resistance of coloured potato cultivars (*Solanum tuberosum* L.): the role of anthocyanins. *Potato Res* 50(1):31–44
- Willson MF, Whelan CJ (1990) The evolution of fruit color in fleshy-fruited plants. *Am Nat* 136(6):790–809
- Xie S, Song C, Wang X, Liu M, Zhang Z, Xi Z (2015) Tissue-specific expression analysis of anthocyanin biosynthetic genes in white- and red-fleshed grape cultivars. *Molecules* 20(12):22767–22780
- Zhang Y, Cheng S, De Jong D, Griffiths H, Halitschke R, De Jong W (2009) The potato R locus codes for dihydroflavonol 4-reductase. *Theor Appl Genet* 119(5):931–937
- Zubko MK, Schmeer K, Gläßgen WE, Bayer E, Seitz HU (1993) Selection of anthocyanin-accumulating potato (*Solanum tuberosum* L.) cell lines from calli derived from seedlings produced by gamma-irradiated seeds. *Plant Cell Rep* 12(10):555–558